(ANPA Conference 2025)
ISSN: 2392-473X(Print), 2738-9537 (Online)

Research Article ©Nepal Physical Society
DOI: https://doi.org/10.3126/jnphyssoc.v11i1.87457

Optical Characterization of Carbon Quantum Dots Under Laser, Magnetic and Heat Treatment

Raman K. Kamat,[1] Surendra Hangsarumba,[1] Santosh K. Das,[1] Suresh P. Gupta,[1] Prakash M. Shrestha,[1] Kishori Yadav,[1] and Saddam H. Dhobi[1, 2, a)]

[1)] *Department of Physics, Patan Multiple Campus, Tribhuvan University, Lalitpur, 44700, Nepal*
[2)] *Central Department of Physics, Tribhuvan University, Kirtipur, Kathmandu, 44600, Nepal*

[a)] *Corresponding author:saddam@ran.edu.np*

Abstract. Carbon quantum dots (CQDs) are emerging nanomaterials with unique optical properties that can be tuned by concentration and external conditions. However, their nonlinear behavior under laser, magnetic, and thermal treatments remains insufficiently explored. Understanding how these factors influence refractive index and transmittance is crucial for advancing their application in optoelectronic devices, sensors, bio-imaging, and energy systems. This work aimed to synthesize and characterize the optical properties of CQDs solution at different concentrations (100%, 50%, 25%, 12.5% by volume) under various environmental conditions, including laser exposure, magnetic field, and heat. CQDs were prepared by mixing citric acid ($C_6H_8O_7$) and thiourea (CH_4N_2S) in a 2:1 weight ratio (1 g: 0.5 g) and heating in a microwave oven (1100 W) at 200–250 ^oC until the mixture formed a dark brown solid. The solid was dissolved in 40 mL distilled water with magnetic stirring for 1 hour and filtered to obtain the 100% concentration solution, which was then diluted to prepare 50%, 25%, and 12.5% solutions. Optical studies were performed using a rotating spectrometer and Theremino spectrometer under the specified environmental conditions. Results showed that the refractive index exhibited nonlinear behavior under laser treatment across all concentrations and was further influenced by magnetic fields, initially increasing to a maximum before decreasing, while at 100% concentration it continuously declined. Temperature also induced nonlinear changes in refractive index, particularly at higher concentrations. Transmittance varied with wavelength (400–700 nm) and treatment: under laser exposure, 100% concentration first decreased then increased, whereas lower concentrations increased steadily. Under magnetic fields, transmittance decreased continuously for 100% and 50% concentrations, but for 25% and 12.5%, it reached a minimum before rising. Temperature similarly affected transmittance, with higher concentrations showing a continuous decrease, 25% showing a minimum before increasing, and 12.5% increasing steadily. These findings highlight the complex interplay of concentration, environmental factors, and wavelength on the optical behavior of CQDs solution.

Received: August 10, 2025; **Revised**: October 22, 2025; **Accepted**: October 22, 2025

Keywords: Carbon quantum dots; refractive index; laser; magnetic field; heat; transmittance

1. INTRODUCTION

Quantum dots (QDs) are semiconductor nanostructures with dimensions typically below 10 nm, whose optical and electronic properties are governed by the quantum confinement effect. Unlike bulk semiconductors, where energy bands are continuous, QDs possess discrete energy levels that allow precise control of their bandgap and photoluminescence simply by adjusting particle size [1] [2]. This tunability, combined with their high quantum yield, surface-dependent emission, and strong nonlinear optical responses, has made QDs promising candidates for optoelectronics, bioimaging, photovoltaics, and nanoscale sensing technologies [3] [4]. Among the various classes of QDs, CQDs have gained increasing attention because they are inexpensive, biocompatible, and environmentally friendly alternatives to heavy-metal-based QDs such as CdSe or PbS. CQDs are typically synthesized from organic precursors such as citric acid, glucose, or thiourea and feature abundant surface functional groups, which improve water solubility, fluorescence, and chemical reactivity [5] [6]. Their electronic structure consists of sp^2/sp^3 hybridized carbon networks, surface defect states, and $\pi-\pi$ conjugated domains that strongly influence photoluminescence, absorption, refractive index, and transmittance. These surface and core states make CQDs highly responsive to external stimuli, offering opportunities for developing tunable optical

devices and nanosensors [6] [7].

Optical characterization is one of the most effective ways to probe the structural and electronic features of QDs. The refractive index (RI), in particular, is a fundamental parameter that describes light–matter interaction, electron density, and polarizability of the medium [8]. Similarly, optical transmittance provides insights into energy band structures, defect states, and scattering mechanisms in nanomaterials. These parameters are not static; they can vary significantly when QDs are subjected to external stimuli such as laser irradiation, magnetic fields, temperature changes, or concentration variations [9] [10]. Previous research has demonstrated that intense laser exposure can alter the electronic structure of QDs by photoinducing surface modifications, enhancing or quenching photoluminescence, and shifting absorption peaks. For example, laser treatment of graphene and carbon-based QDs has been reported to induce structural reordering and functional group transformations, leading to nonlinear changes in optical properties [11] [5]. Similarly, magnetic fields can strongly influence QDs through the magneto-optic effect, where external fields perturb excitonic states or induce Zeeman splitting, thus modifying refractive index and absorption spectra [12] [13]. Temperature also plays a critical role; heating can enhance carrier mobility or induce desorption of surface ligands, leading to bandgap shifts and variations in refractive index or transmittance [2]. In addition, concentration directly affects optical density, aggregation, and inter-dot interactions, which can result in quenching effects or nonlinear optical responses [4].

Despite these advances, most studies to date have focused either on a single type of external perturbation or on inorganic QDs such as CdSe and GaAs. For instance, Poudyal et al. investigated size-dependent fluorescence of CdSe QDs, while other groups have studied magneto-optic effects in doped QDs [14]. Comparatively fewer studies have systematically examined how carbon-based QDs respond simultaneously to laser, magnetic, thermal, and concentration variations, especially in terms of refractive index and transmittance. This gap limits our understanding of the fundamental optoelectronic resilience and tunability of CQDs under realistic laboratory and environmental conditions.

2. EXPERIMENTAL METHODS

2.1 Synthesis of Carbon Quantum Dots (CQDs)

Citric acid (C) of 1± 0.01 g and thiourea (U) of 0.5± 0.01 g was measured using digital weighting device of least count ± 0.01 and the measured amount of citric acid and thiourea was mixed in 2:1 ratio by weight in 250 ml borosilicate glass. The mixture was placed in a microwave oven of 1100 W and heated of 200–250 ^{o}C until the mixture transformed into a dark brown-colored solid. The mixture was cooled naturally and cooled mixture was diluted with 40ml of water and filtered. The sketch of experimental diagrams is shown in figure 1. The filtered solution is known as sample of 100% and for 50%, 25% and 12.5% the 100% sample was diluted. To prepared CQDs solution we follow the methodology [15] [16]. The prepared sample was tested at different condition using rotating spectrometer and theremino spectrometer.

To study the refractive index of CQDs solutions at different concentrations and environmental conditions, a rotating spectrometer was used with the minimum deviation method, employing a hollow prism spectrometer and a sodium light source (589 nm) as the monochromatic beam. For calibration, the prism angle was determined using sodium light after warming it for about five minutes, ensuring proper leveling with a spirit level, maintaining a dark environment for accurate readings, and minimizing errors. The refractive index of CQDs was then obtained using equation (1) below.

$$\mu = \frac{\sin\left(\frac{A+D_{\min}}{2}\right)}{\sin\left(\frac{A}{2}\right)} \tag{1}$$

where μ is the refractive index, D_{min} is the minimum deviation, and A is the prism angle. The transmittance properties of CQDs solutions with varying concentrations and environmental conditions were studied using a Theremino spectrometer, which provides real-time monitoring of light intensity from the UV to the infrared range; however, only the visible spectrum (400–700 nm) was considered in this work. The analysis is based on the Beer–Lambert law, which relates the transmittance of light through a medium to its intrinsic properties and is mathematically expressed as:

$$T = \frac{I}{I_0} \times 100 \tag{2}$$

where T is the transmittance, I is the transmitted light intensity, I_0 is the incident light intensity. The transmittance of the sample was performed using a self-made Theremino spectrometer, which operates within the visible wavelength range (400 nm to 700 nm). The design and components of the Theremino spectrometer are illustrated in Figure 2. The system utilizes the Theremino−Spectrometer−V4.0 software, which facilitates data acquisition, spectral analysis, and calibration. This software allows for precise measurement of the optical properties, ensuring accurate characterization. The detector used in Webcam (Full HD 1080P), LED sources (60000 lux), sample holder is cuvette of 3 mL and the distance between sources and sample is 5 cm and that of

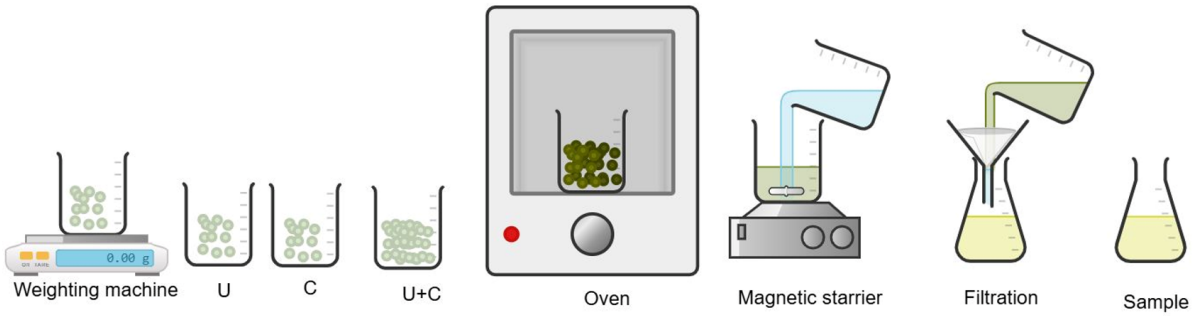

FIGURE 1: Laboratory Preparation of Synthesize carbon Quantum Dots.

sample and webcam is 3 cm. All setup is done a black box where the external light is not entered the inner side of the spectrometer. Using this setup of some study is done to study the optical properties of water [17] [18] [19]. The ready setup was calibrated using the solvent on which solute is dissolved we used solvent as distilled water.

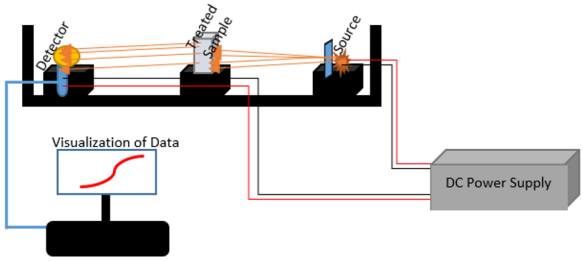

FIGURE 2: Experimental arrangement for plasma generation followed by sample treatment and transmittance measurements.

2.2 Different testing environmental condition

In this study, three environmental conditions were considered for treating CQDs solutions at different concentrations. As shown in Figure 3(a), the solutions were exposed to laser irradiation with a power of 100 mW and wavelength of 532 nm. Figure 3(b) presents the heat treatment of CQDs solutions at temperatures of 30 ^{o}C, 45 ^{o}C, and 60 ^{o}C, while Figure 3(c) illustrates the effect of magnetic treatment under field strengths of 0.5 T, 1.0 T, and 1.5 T. The treated sample was palce on hollow prism and with calibration of rotating spectrometry the sample is for each condition, the CQDs solution was placed on the stand, and readings were recorded both with and without the sample using the main and vernier scales. In the case of laser treatment, each concentration of CQDs

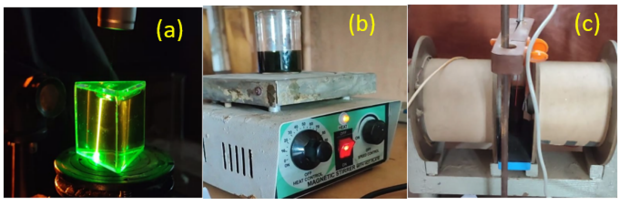

FIGURE 3: Treatment of QDs solution under three environment condition.

solution was exposed for 1, 2, 3, and 4 minutes, after which refractive index and transmittance measurements were taken. For magnetic treatment, the samples were subjected to field strengths of 0.5 T, 1.0 T, and 1.5 T for 5 minutes, followed by the same measurements. Similarly, for heat treatment, CQDs solutions of different concentrations were heated to 30 ^{o}C, 45 ^{o}C, and 60 ^{o}C, and the corresponding refractive index and transmittance values were recorded.

3. RESULTS AND DISCUSSION

3.1 Effect of laser, magnetic field and heat on refractive Index of different concentration of QDs solution

Figure 4 shows the effect of laser on refractive index of CQDs solution at different concentrations (100%, 50%, 25%, and 12.5%) with laser treatment 0 to 4 minutes. The refractive index of CQDs solution has nonlinear nature with treated time of sample of different concentration. The refractive index of all sample found higher than refractive index of water. The refractive index of 12.5 % concentrations was found higher than other concentrations % of CQDs samples while 25% is lower than other concentrations % of CQDs samples. The nonlinear behavior may be attributed to the higher density of CQDs,

which leads to more uniform absorption and scattering, thereby preventing rapid structural alteration. In contrast, the 50% concentration displays an initial drop in refractive index at 1 minute, followed by a gradual rise until 3 minutes and then a subsequent decline at 4 minutes. This indicates a more complex interaction, likely resulting from intermediate-level CQD clustering or partial photo-induced restructuring.

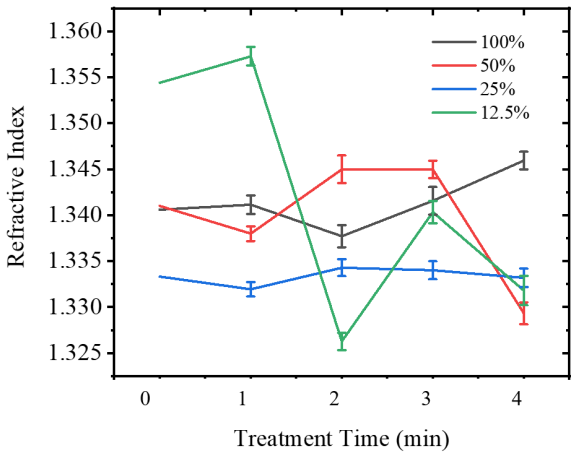

FIGURE 4: Effect of laser treated time on refractive index of CQDs solution at different concentrations (100%, 50%, 25%, 12.5%).

The 25% concentration of CQDs solution remains comparatively stable throughout the laser exposure period, with only minor fluctuations in refractive index, indicating moderate resilience to laser-induced effects. However, the 12.5% concentration of CQDs solution shows the most dynamic and erratic behavior. At 1 minute of exposure, there is a sharp increase in refractive index, which is followed by a significant drop at 2 minutes. A slight increase is again observed at 3 minutes before another decline at 4 minutes. This highly unstable trend at lower concentration levels can be attributed to several factors: with fewer CQDs present in solution, the interaction of individual particles with the incident laser beam becomes more pronounced, leading to rapid energy absorption, localized heating, and potential photochemical or structural changes. These processes can include photo-oxidation, disintegration of surface functional groups, or aggregation phenomena, all of which directly impact the optical path length and polarizability of the medium, thereby altering the refractive index. Higher concentrations of CQDs solution are more resistant to laser-induced changes due to denser packing and mutual shielding effects, while lower concentrations exhibit enhanced sensitivity, likely due to the higher availability of surface-active sites and increased quantum confinement effects under laser irradiation. The refractive index values obtained in this study (1.326–1.361) are comparatively low in comparision to the AA-CQDs reported in ACS Nano that are dense, crystalline materials with intrinsically high refractive index (1.7–2.15) [20] this is because we have calculated the refractive index of CQDs solution.

The effects of external magnetic fields on the refractive index of CQDs solution at varying concentrations is shown in figure 5. The observation shows in refractive index across different concentrations (100%, 50%, 25%, and 12.5%) highlight the magneto-optical sensitivity of CQDs in solution and their complex interaction with magnetic stimuli. At a concentration of 100%, the refractive index shows a slight and nearly linear decrease with increasing magnetic field strength, suggesting that highly concentrated CQDs in solution maintain relatively stable structural and optical properties even under external magnetic influence. This minor change may be due to the limited ability of the magnetic field to perturb the dense network of CQDs in solution, where strong inter-dot interactions and compact surface states reduce susceptibility to reorientation or magnetic alignment [21] [22]. In contrast, the 50% concentration reveals a more

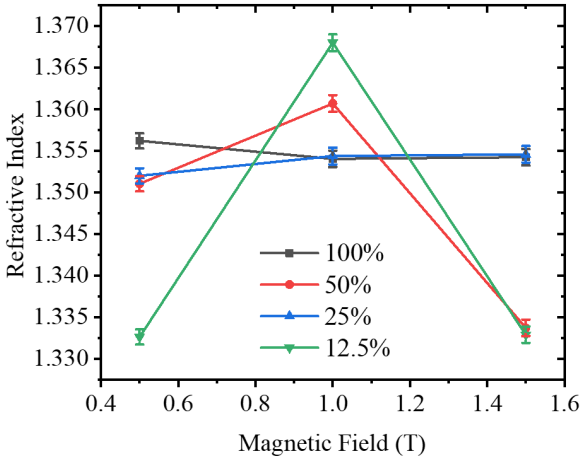

FIGURE 5: Refractive index of CQDs solution when sample was treated 5 minutes in magnetic field.

pronounced response, with a visible drop in refractive index particularly at 1.0 T, followed by a mild recovery or plateauing at 1.5 T. This non-linear behavior indicates that at intermediate concentrations, the balance between magnetic alignment forces and inter-particle interactions leads to transient optical reordering, possibly involving minor orientation shifts in surface dipoles or changes in charge distribution. The effect becomes more dramatic at 25% and 12.5% concentrations of CQDs in solution. At 25%, the refractive index decreases consistently with magnetic field strength, indicating progressive magnetic field-induced structural modulation. Meanwhile, the 12.5% concentration exhibits the highest sensitivity: the refractive index shows abrupt variations across all mag-

netic strengths, pointing to significant rearrangement or reorientation of CQDs in solution due to reduced particle-particle interactions and increased exposure of individual CQDs in solution to the field [23]. These variations can be attributed to the magneto-optic effect, where the presence of a magnetic field alters the light propagation characteristics in a medium by influencing the electronic environment of the material. In CQDs solution, this may manifest through Zeeman splitting of energy levels, magnetic field-induced realignment of surface dipoles, or changes in electronic transitions, all of which contribute to refractive index modulation. The response is more noticeable at lower concentrations, where isolated CQDs solution with high surface-to-volume ratios exhibit greater sensitivity to external perturbations. Conversely, in densely packed systems, the magnetic influence is dampened by collective stabilization effects. The refractive index of CQDs solution was systematically investigated at three different temperatures (30 ^{o}C, 45 ^{o}C, and 60 ^{o}C) across four volumetric concentrations (100%, 50%, 25%, and 12.5%) shown in figure 6. The results reveal that both temperature and concentration strongly influence the refractive index, but the nature of the variation differs with particle density. At 100% concentration, the refractive index shows a steady increase with temperature, rising from 1.348 at 30 ^{o}C to 1.361 at 60 ^{o}C. This monotonic trend indicates that densely packed CQDs solution exhibit strong inter-dot interactions and structural stability under heating. Thermal excitation likely enhances the polarizability of surface states and slightly modifies interparticle spacing, leading to an overall increase in optical density. The absence of nonlinear fluctuations suggests that high concentration CQDs in solution are thermally stable and resistant to large-scale surface or structural disruption. At

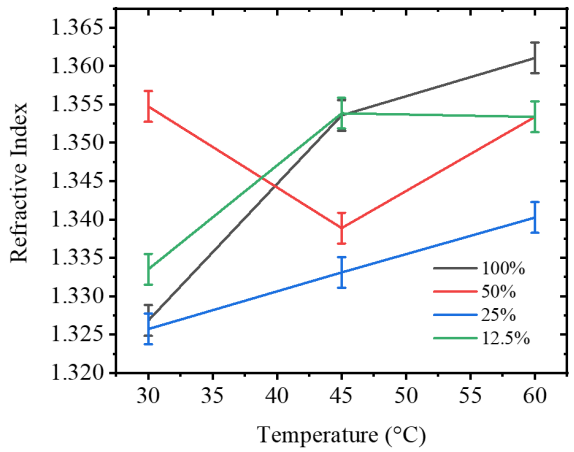

FIGURE 6: Effect of temperature on refractive index of CQDs solution of different concentration.

50% concentration, a nonlinear variation is observed. The refractive index decreases at 45 ^{o}C compared to 30 ^{o}C, before partially recovering at 60 ^{o}C. This dip may originate from surface restructuring or partial desorption of weakly bound functional groups upon moderate heating, which reduces the medium's polarizability. The subsequent stabilization at higher temperature indicates that the system reorganizes into a thermodynamically favorable configuration, minimizing further refractive index fluctuations. At 25% concentration, the refractive index increases sharply between 30 ^{o}C and 45 ^{o}C, followed by a plateau toward 60 ^{o}C. This behavior suggests that initial heating activates surface dipoles or enhances charge redistribution at CQDs interfaces in solution, thereby increasing polarizability. However, further heating does not lead to continued enhancement, indicating a saturation effect where available active sites or structural rearrangements have stabilized. The most distinct behavior occurs at 12.5% concentration, where the refractive index starts at the lowest baseline but increases consistently across the entire temperature range. The continuous rise reflects the dominance of individual CQD present in solution response rather than collective inter-dot shielding. At such dilute conditions, surface states are highly exposed, and even small thermal perturbations can enhance dipole orientation and polarizability, leading to a pronounced sensitivity to temperature.

3.2 Effect of laser, magnetic field and heat on transmittance of different concentration of QDs solution

The transmittance spectra of CQDs solution at 100 % concentration under varying durations of laser exposure reveal distinct changes in their optical behavior shown in figure 7. As illustrated in the figure 7(a), the CQD solution exposed for 1 minute shows the highest transmittance across the visible range, particularly beyond 650 nm, where transmittance rises sharply. This behavior is typical for CQDs solution, which strongly absorb in the 400–600 nm region and become increasingly transparent at longer wavelengths. As the duration of laser exposure increases to 2, 3, and 4 minutes, a gradual reduction in transmittance is observed throughout the spectrum, with the 4- minute exposure showing the lowest values. This indicates that prolonged laser irradiation enhances the CQDs in solution ability to absorb light. The underlying mechanism is likely due to photo induced structural or surface modifications, such as the formation of defect states, oxidation of surface groups, or changes in particle size and energy band structure. These changes increase the density of localized energy states and facilitate more effective photon absorption. Thus, laser exposure time serves as a tunable parameter to modify the optical properties of CQDs solution, even at full (100 %) concentration, which is particularly relevant for applications requir-

ing controlled light absorption and transmittance behavior.

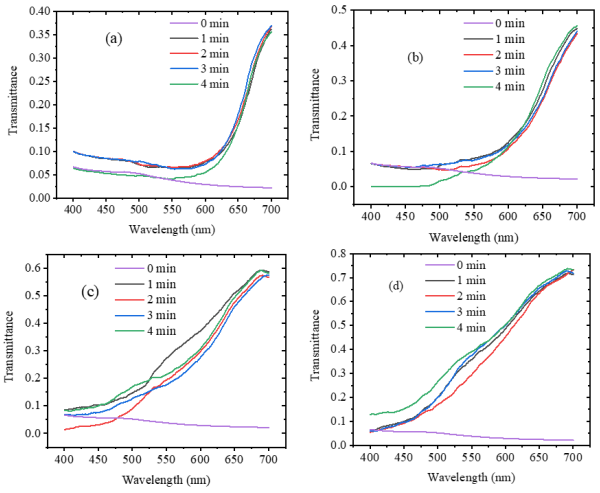

FIGURE 7: Transmittance spectra of CQDs solution at (a) 100 %, (b) 50 %, (c) 25 % and (d) 12.5 % concentration under different laser treatment times.

Also figure 7(b) show the transmittance of 50 % CQDs solution and exhibit similar overall trends to the 100 % concentration case (Figure 7a), with transmittance increasing beyond 650 nm and decreasing progressively with increased thermal exposure time. However, the absolute transmittance values at 50 % concentration are higher across the visible spectrum compared to those at 100 %, due to the lower particle density and reduced optical absorption in the diluted solution. The optical response of CQDs solution of 25 % concentration was also evaluated to understand how dilution influences their transmittance behavior under thermal exposure as shown in figure 7(c). As shown in Figure 7(c), the spectra display a consistent trend with the previously studied 100 % and 50 % concentrations: transmittance increases with wavelength, particularly beyond 600 nm. However, at 25 % concentration, the transmittance values are significantly higher across the entire spectral range, with maximum values nearing 0.6, which reflects the expected outcome due to reduced CQD density in the diluted solution.

Figure 7(d) presents the transmittance spectra of CQDs solution of 12.5 % concentration subjected to different durations of laser exposure. Overall, the transmittance increases steadily with wavelength across all samples, with maximum values approaching 0.7–0.75 near 700 nm, which is consistent with the behavior observed in more concentrated samples. In contrast to higher concentrations where a consistent decrease in transmittance was observed with longer laser exposure, the 12.5 % samples show a more irregular trend. Notably, the 4 minutes laser-exposed sample exhibits the highest transmittance throughout much of the visible spectrum, while the 2-minute sample appears to have the lowest. The 1 minute and 3 minutes samples lie in between, with overlapping portions in some spectral regions. This variation suggests that at very low concentrations, the laser-induced modifications to CQDs solution may have less predictable optical effects, possibly due to reduced interparticle interaction, minimized scattering, or limited absorption depth in the dilute medium.

Across all tested concentrations from 100 % to 12.5 % laser exposure time consistently influences the transmittance of CQDs solution. At higher concentrations (100 %, 50 %), increased exposure time leads to a clear reduction in transmittance due to enhanced absorption from photo-induced surface modifications and defect generation. At moderate concentrations (25 %), this trend remains visible but slightly attenuated. However, at low concentrations (12.5 %), the response becomes more variable, and in some cases, transmittance may even increase with longer exposure. This suggests that while laser-induced structural changes still occur, their impact on optical properties is significantly moderated by the reduced quantum dot density. These findings emphasize that both concentration and exposure duration play key roles in determining the optical behavior of CQDs. In dilute systems, the effects of laser interaction are less predictable and possibly more sensitive to localized conditions such as particle size distribution or laser beam uniformity. This highlights the importance of optimizing laser parameters for specific CQD concentrations when designing optical materials or devices.

The transmittance of 100 % concentration CQDs solution under different magnetic field strengths (0.5 T, 1.0 T, and 1.5 T) and without magnetic field treatment reveal a clear decreasing trend in 400–700 nm as shown in figure 8. For all samples, the transmittance is highest in the lower wavelength range near 400 nm and gradually decreases toward the longer wavelengths, indicating stronger light absorption in the red region compared to the blue. The untreated CQDs and those subjected to magnetic field treatment exhibit similar overall profiles, but subtle differences can be observed in the magnitude of transmittance. In the shorter wavelength region (below 500 nm), the differences between treated and untreated samples are minimal, suggesting that the magnetic field has a limited influence on high-energy photon interaction. However, in the mid to longer wavelength range (500–700 nm), samples treated with magnetic fields particularly at higher strengths show slightly reduced transmittance compared to the untreated sample, implying enhanced absorption or scattering under magnetic influence. This reduction may be attributed to magnetic field–induced alignment or clustering of CQDs, which can modify their optical path and interaction with light, thereby enhancing photon trapping and reducing transmittance

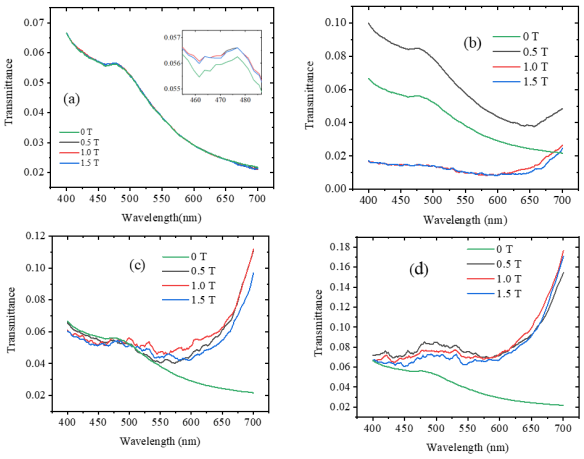

FIGURE 8: Transmittance spectra of CQDs solution at (a) 100 %, (b) 50 % , (c) 25 % and (d) 12.5 % concentration at different magnetic field.

The transmittance of 50 % concentration CQDs solution under magnetic fields of 0.5 T, 1.0 T, and 1.5 T show in figure 8(b) has a distinct spectral behavior compared to the 100 % concentration samples. In all three cases, the transmittance is highest in the shorter wavelength region near 400 nm, followed by a gradual decrease towards the mid-visible range (500–600 nm), and then a slight rise beyond 650 nm. The curves for 1.0 T and 1.5 T are closely aligned across the spectrum, both showing consistently lower transmittance than the 0.5 T sample, particularly in the range from 450 nm to 650 nm. The transmittance of solution in absence of magnetic field is lower than 0.5 T while higher than 1.0 T and 1.5 T cases. When compared to the 100 % concentration of CQDS solution, the 50 % concentration spectra exhibit overall lower transmittance values for the higher magnetic field strengths, suggesting that at reduced CQDs concentration in solution as shown in figure 8(b), the magnetic field effect becomes more dominant relative to the base scattering and absorption.

This indicates a possible interplay between particle density and magnetic alignment efficiency, where fewer particles allow the magnetic field to influence a greater proportion of the system's optical pathways. The transmittance of 25 % concentration CQDs solution under magnetic fields of 0.5 T, 1.0 T, and 1.5 T demonstrate a characteristic wavelength dependence which is also compare with 0 T as shown in figure 8(c). Across all field strengths, the transmittance is highest in the short-wavelength region around 400 nm, then decreases progressively through the visible range, reaching a minimum between 550-600 nm, before showing a modest increase beyond 650 nm. The three field strength curves maintain nearly identical profiles throughout the spectrum, with only minimal separation between them. In the blue-green region (450-550 nm), the transmittance declines steadily from its peak at 400 nm, with the 1.0 T and 1.5 T curves exhibiting marginally lower values than the 0.5 T reference. This difference, while small, is most noticeable in the 500-550 nm range. The curves converge again in the orange-red region (600-700 nm), where all three field conditions show comparable transmittance values with a slight upward trend toward longer wavelengths.

The transmittance of 12.5 % concentration CQDs solution under magnetic fields of 0 T 0.5 T, 1.0 T, and 1.5 T exhibit minimal variation across all field strengths as shown in figure 8(d). The curves for all three magnetic field conditions nearly overlap throughout the entire visible spectrum (400-700 nm), maintaining consistent transmittance values ranging from approximately 0.18 at 400 nm to 0.06 at 700 nm. The spectral profile shows highest transmittance in the violet-blue region (400-450 nm), followed by a gradual decline through the green-yellow wavelengths (500-550 nm), reaching a minimum around 550-600 nm. Beyond 600 nm, the transmittance values stabilize with only a slight decrease toward the red end of the spectrum. The curves for 1.0 T and 1.5 T magnetic fields show negligible deviation from the 0.5 G baseline, with differences smaller than the line widths throughout the measured range. This indicates that at this low concentration, the magnetic field has virtually no detectable effect on the optical transmittance properties of the CQD solution.

At 100 % concentration of CQDs solution, the strongest field effects emerge, showing 20 % transmittance suppression at 1.5 T with a pronounced dip in the 450-600 nm range. The 50 % samples display similar but attenuated behavior (15 % suppression), while maintaining comparable spectral features. By contrast, 25 % concentration CQDs solution show minimal field sensitivity ($<$5 % variation) and a much shallower transmission dip, indicating weakened interparticle interactions. The most dilute system (12.5 %) demonstrates complete field independence with featureless, high-transparency spectra. This progression reveals a critical transition between collective ($\geq$50 %) and single-particle ($\leq$25 %) regimes, where magnetic effects require sufficient particle density for dipole coupling. The concentration-dependent modulation depth and spectral signatures directly correlate with interparticle distances, suggesting that applications requiring field-responsive optics should employ $\geq$50 % CQDs solution, while $\leq$25 % systems are better suited for stable, environment-insensitive applications. These systematic trends provide clear design principles for tailoring CQD-based optical materials to specific functional requirements.

The general spectral shape remains consistent, the presence of a magnetic field subtly modifies the optical properties, with stronger fields showing more pronounced deviations from the untreated state, especially in the red and

near-infrared edges of the visible spectrum. Transmittance varies systematically with increasing magnetic field in both front and back geometries, suggesting magneto-optical modulation of optical properties [24]. Similarly, in our results, although the variations are smaller, different magnetic field strengths (0.5 T, 1.0 T, 1.5 T) subtly alter the transmittance curve of quantum dots across the visible spectrum compared to the untreated case.

The transmittance of 100 % concentration CQDs solution at different temperatures (30 ^{o}C, 45 ^{o}C, and 60 ^{o}C) reveal a clear temperature-dependent optical response as shown in figure 9. At 30 ^{o}C (room temperature), the sample exhibits the highest transmittance (0.065 at 400 nm), which gradually decreases with increasing wavelength, indicating stronger absorption in the shorter wavelength region due to $\pi - \pi^*$ transitions in the graphitic domains of CQDs solution as shown in figure 9(a). When the temperature is raised to 45 ^{o}C, the transmittance drops significantly (0.012 at 400 nm), with a relatively flatter spectrum, suggesting enhanced broadband absorption caused by thermal broadening and increased phonon-assisted transitions. At 60 ^{o}C, the transmittance approaches zero across the visible range, indicating almost complete suppression of transmitted light due to strong absorption and possible aggregation of CQDs solution, which increases scattering. This overall reduction in transmittance with temperature can be attributed to thermal bandgap narrowing, enhanced electron–phonon interactions, and temperature-induced surface or structural changes, all of which increase the light–matter interaction efficiency of the CQDs solution. For the 50 % concentration CQDs solution, the transmittance at 30 ^{o}C, 45 ^{o}C, and 60 ^{o}C exhibit a different temperature-dependent behaviour compared to the 100 % concentration sample as shown in figure 8(b). At 30 ^{o}C, the transmittance starts around 0.065 at 400 nm and decreases steadily to 0.022 near 650 nm, showing a pronounced absorption in the shorter wavelength region as shown in figure 9(b). At higher temperatures (45 ^{o}C and 60 ^{o}C), the transmittance curves almost overlap, starting near 0.10 at 400 nm and declining more gradually, with a slight increase after 650 nm

When comparing the 50 % with 100 % concentrations CQDs solution, a clear relationship between concentration and temperature is observed. At the higher concentration (100 %), increasing temperature leads to a significant drop in transmittance, with the 60 ^{o}C spectrum approaching near-zero values across the visible range, suggesting strong light absorption and possible particle aggregation. The temperature-dependent transmittance behavior of 25% CQD solutions reveals significantly diminished thermal sensitivity compared to more concentrated systems as shown in figure 9(c). At this intermediate dilution, the spectra exhibit only modest changes (5-8% maximum transmittance reduction) when heated from 30 ^{o}C to 60 ^{o}C, with nearly identical curves observed at 45 ^{o}C and 60 ^{o}C. This minimal response contrasts sharply with the strong thermal modulation seen in 100% concentration CQDs solution and the intermediate effects in 50% solutions. The near-overlap of 45 ^{o}C and 60 ^{o}C spectra particularly highlight how dilution decouples optical properties from thermal energy, as the solution transitions from ensemble-dominated to single-particle behavior. These findings establish 25% concentration as a practical boundary for applications requiring temperature-stable CQDs solution performance, while demonstrating how systematic dilution can progressively suppress thermal modulation effects observed in more concentrated systems. The results complete the observed progression from strongly temperature-dependent (100 %) to moderately responsive (50 %) and finally to nearly temperature-invariant (25 %) optical behavior in CQD solutions.

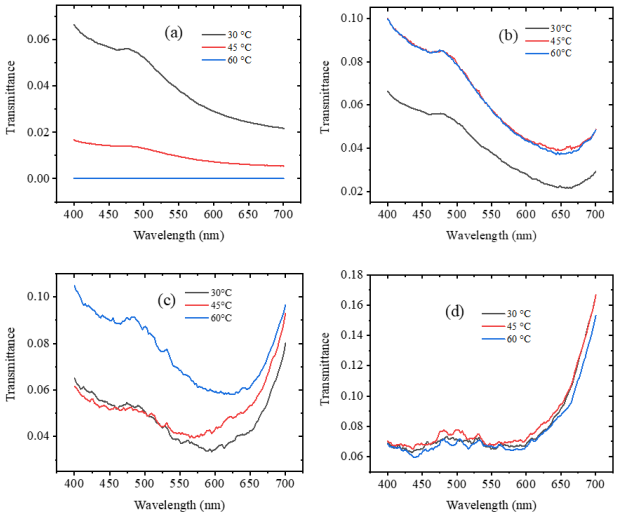

FIGURE 9: Transmittance of CQDs solution at (a) 100 %, (b) 50 %, (c) 25 % and (d) 12.5 % concentration at different temperature.

The transmittance of 12.5 % concentration CQDs solutions demonstrate complete temperature stability across the tested range (30 ^{o}C-60 ^{o}C) as shown in figure 9(d), marking the extreme dilution limit where thermal effects become negligible. At this ultralow concentration, all temperature curves (30 ^{o}C, 45 ^{o}C, and 60 ^{o}C) perfectly overlap, maintaining identical transmittance values from 400-700 nm with a characteristic smooth decline from 0.18 (400 nm) to 0.06 (700 nm). Compared to even the 25% solution, which showed minimal but detectable thermal modulation, the 12.5% system represents true temperature-independent performance - all thermal curves collapse to a single trace, establishing this as the fundamental dilution limit for erasing temperature sensitivity in CQD suspensions. These results complete the concentration-dependent progression from strongly

thermally responsive (100%) to completely thermally invariant (12.5%) behavior, providing clear design rules for applications requiring either tunable or stable optical properties across temperature ranges. In addition, this work has limitations in terms of comparison and validation with previous studies due to the specific focus of our research, namely the effects of CQD solutions under laser, magnetic field, and heat on refractive index and transmittance.

4. CONCLUSION

The study of CQDs using its solution with distill water under varying concentrations and external stimuli laser exposure, magnetic fields, and thermal treatment—reveals a clear correlation between concentration and optical behavior. High-concentration CQDs solution(100%) exhibited minimal variations in refractive index and transmittance, attributed to strong inter-dot interactions, dense packing, and shielding effects that enhance structural and photothermal stability. Conversely, low-concentration CQDs solution (12.5%) displayed the highest sensitivity and irregular optical responses, driven by their large surface-to-volume ratio and reduced shielding, making them highly responsive to external perturbations. Intermediate concentrations (25% and 50%) showed moderate, often nonlinear responses, balancing stability with environmental sensitivity. Laser exposure induced wavelength-dependent modulation, magnetic fields reduced overall transmittance through magneto-optic interactions, and thermal treatment caused redshifts and suppression due to electronic structure alterations. These outcomes suggest that high-concentration CQDs solution are promising for stable optical devices, whereas low-concentration CQDs solution are better suited for sensing applications where responsiveness is desired. Future work should focus on advanced spectroscopic techniques to correlate optical responses with structural and electronic modifications, explore synthesis strategies for precise tuning, and expand investigations to wider spectral ranges. Device integration and long-term performance testing will be essential for translating laboratory findings into real-world applications across optical communication, sensing, and bioimaging.

ACKNOWLEDGMENTS

We would like thank the Department of Physics, Patan Multiple Campus, and the Central Department of Physics, Tribhuvan University, for providing facilities, guidance, and support. We also grateful to the Association of Nepali Physicists in America (ANPA) and the Nepal Physical Society (NPS) team for their encouragement and valuable insights.

EDITORS' NOTE

This manuscript was submitted to the Association of Nepali Physicists in America (ANPA) Conference 2025 for publication in the special issue of the Journal of Nepal Physical Society.

REFERENCES

1. A. P. Alivisatos, "Semiconductor clusters, nanocrystals, and quantum dots," Science **271**, 933–937 (1996).
2. A. Loskutova, A. Seitkali, D. Aliyev, and R. Bukasov, "Quantum dot-based luminescent sensors: Review from analytical perspective," Int. J. Mol. Sci. **26**, 6674 (2025).
3. D. Bera, L. Qian, T. K. Tseng, and P. H. Holloway, "Quantum dots and their multimodal applications: A review," Materials **3**, 2260–2345 (2010).
4. K. Hola, Y. Zhang, Y. Wang, E. P. Giannelis, R. Zboril, and A. L. Rogach, "Carbon dots—Emerging light emitters for bioimaging, cancer therapy and optoelectronics," Nano Today **9**, 590–603 (2014).
5. M. K. Kumawat, M. Thakur, R. B. Gurung, and R. Srivastava, "Graphene quantum dots from *Mangifera indica*: Application in near-infrared bioimaging and intracellular nanothermometry," ACS Sustain. Chem. Eng. **5**, 1382–1391 (2017).
6. M. Langer, M. Paloncýová, M. Medveď, M. Pykal, D. Nachtigallová, B. Shi, and M. Otyepka, "Progress and challenges in understanding of photoluminescence properties of carbon dots based on theoretical computations," Appl. Mater. Today **22**, 100924 (2021).
7. R. Wang, K. Q. Lu, Z. R. Tang, and Y. J. Xu, "Recent progress in carbon quantum dots: Synthesis, properties and applications in photocatalysis," J. Mater. Chem. A **5**, 3717–3734 (2017).
8. M. Born and E. Wolf, "Principles of optics: Electromagnetic theory of propagation, interference and diffraction of light," Elsevier (2013).
9. X. Chen, X. Zhang, and F. G. Wu, "Ultrasmall green-emitting carbon nanodots with 80% photoluminescence quantum yield for lysosome imaging," Chin. Chem. Lett. **32**, 3048–3052 (2021).
10. E. Karpushkin, E. Kharochkina, E. Mesnyankina, O. Zaborova, and V. Sergeyev, "Optical and sensing properties of carbon colloidal particles based on (thio)urea and citric acid: Effect of the components ratio," Physchem **3**, 92–109 (2023).
11. J. Wang, G. Liu, K. Cham-Fai Leung, R. Loffroy, P. X. Lu, and Y. X. J. Wang, "Opportunities and challenges of fluorescent carbon dots in translational optical imaging," Curr. Pharm. Des. **21**, 5401–5416 (2015).
12. J. K. Furdyna, "Diluted magnetic semiconductors," J. Appl. Phys. **64**, R29–R64 (1988).
13. S. Nandi, S. N. Majji, and A. Misra, "Effects of optical and magnetic fields on the electrical characteristics of colloidal graphene quantum dots," RSC Adv. **6**, 40577–40584 (2016).
14. U. Poudyal, C. M. Adhikari, N. H. Makani, B. R. Gautam, and T. Neupane, "Size-dependent fluorescence properties of CdSe quantum dots," Solid State Commun. 115993 (2025).
15. V. B. Kumar, S. K. Mirsky, N. T. Shaked, and E. Gazit, "High quantum yield amino acid carbon quantum dots with unparalleled refractive index," ACS Nano **18**, 2421–2433 (2024).

16. H. Li, Z. Kang, Y. Liu, and S. T. Lee, "Carbon nanodots: Synthesis, properties and applications," J. Mater. Chem. **22**, 24230–24253 (2012).
17. S. H. Dhobi, J. J. Nakarmi, K. Yadav, and S. P. Gupta, "Optical properties of atmospheric air molecules," J. Sci. Tech. Inf. Tech. Mech. Opt. **24**, 375–383 (2024).
18. S. H. Dhobi, J. J. Nakarmi, R. Waiba, B. Koirala, K. Yadav, S. P. Gupta, and L. D. Lemle, "Magneto-optical properties of water and saltwater in presence of a magnetic field," J. Phys.: Conf. Ser. **2540**, 012002 (2023).
19. B. Karki, S. H. Dhobi, I. Dhobi, D. Pandey, and B. K. Pandey, "Study the optical properties of drinking water supply by KUKL and KVWSIP in Kathmandu Valley," Discover Water **1**, 6 (2021).
20. A. K. Zvezdin and V. A. Kotov, "Modern magnetooptics and magnetooptical materials," CRC Press (1997).
21. X. Xu, R. Ray, Y. Gu, H. J. Ploehn, L. Gearheart, K. Raker, and W. A. Scrivens, "Electrophoretic analysis and purification of fluorescent single-walled carbon nanotube fragments," J. Am. Chem. Soc. **126**, 12736–12737 (2004).
22. A. K. Singh, P. Barik, and B. Ullrich, "Magneto-optical controlled transmittance alteration of PbS quantum dots by moderately applied magnetic fields at room temperature," Appl. Phys. Lett. **105**, (2014).
23. S. Singh, "Refractive index measurement and its applications," Phys. Scr. **65**, 167 (2002).
24. R. Tabaraki and N. Sadeghinejad, "Microwave assisted synthesis of doped carbon dots and their application as green and simple turn off–on fluorescent sensor for mercury (II) and iodide in environmental samples," Ecotoxicol. Environ. Saf. **153**, 101–106 (2018).